Pressure and Temperature Dependence of the Static Dielectric Constants and Raman Spectra of TiO_2 (Rutile)*

G. A. Samara and P. S. Peercy
Sandia Laboratories, Albuquerque, New Mexico 87115
(Received 26 July 1972)

The effects of temperature [(4–500)°K] and hydrostatic pressure (0–4 kbar) on the static dielectric constants ϵ_a and ϵ_c and on the frequencies of the four Raman-active phonons B_{1g}, E_g, A_{1g}, and B_{2g} of single-crystal rutile were investigated. The temperature and pressure dependence of the frequency of the infrared-active soft ferroelectric (FE) mode A_{2u} were deduced from the dielectric-constant data. The Grüneisen parameter γ of each of the modes was determined. Particularly important are the results that $\gamma(A_{2u})$ is large and increases with decreasing temperature—unique properties of the FE mode—and that $\gamma(B_{1g})$ is relatively large and negative. This latter result, which is in agreement with an earlier measurement, may be significant from the standpoint of a pressure-induced phase transition in rutile. The temperature and pressure results are combined with thermal expansion and compressibility data to evaluate the pure-volume and pure-temperature contributions to the isobaric temperature dependence of each of the frequencies and dielectric constants. The results yield some important conclusions about the lattice dynamics of rutile. The pure-temperature contribution arises from cubic and quartic anharmonicities. It plays a dominant role in determining the anharmonic self-energy shift of the FE mode and accounts for 20% of the mode energy at 300 °K. The Szigeti effective ionic-charge ratio for rutile is found to be $e^*/e = 0.64$ at 4 °K and 0.62 at 296 °K. These results are discussed briefly.

I. INTRODUCTION

The tetragonal form of titanium dioxide (TiO_2, rutile) is a crystal of considerable fundamental and applied interest. Its dielectric,[1] optical,[2,3] and elastic[4] properties have been subjects of recent interest. Very recently, a detailed experimental and theoretical study of its lattice dynamics, based on coherent inelastic neutron scattering measurements, was reported by Traylor *et al.*[5]

Among rutile's most interesting properties are its high-static dielectric constants which increase with decreasing temperature obeying a modified Curie–Weiss law. It is now known[2,5] that this behavior is associated with the presence in rutile of a soft long-wavelength transverse-optic (TO) phonon (the so-called ferroelectric mode), as in the case of the ferroelectric (FE) perovskites. The frequency of this mode decreases with decreasing temperature. However, dielectric measurements down to ~1 °K do not show any evidence for a transition, and so like some perovskites, notably $KTaO_3$, rutile can be classified as an incipient ferroelectric. Another pertinent feature is that the Ti-O framework in rutile is very similar to that in the perovskites in that it consists of Ti ions octahedrally surrounded by oxygens.

In rutile, as well as in the perovskites, anharmonicities resulting from interactions among the normal modes of vibration play important roles in the lattice dynamics of these crystals. These anharmonic effects cause the energies (or frequencies) of the normal modes to be temperature dependent. This temperature dependence arises in two different ways. First, there is a pure-volume effect associated with the thermal expansion of the crystal. Second, there is a pure-temperature effect which is present even when the crystal is held at constant volume. Isobaric measurements of the temperature dependence of the phonon frequencies and other associated physical properties yield changes due to the combination of the two effects. However, measurements of both the pressure and temperature dependence of these properties allow a separation of the volume-dependent and volume-independent contributions, and under suitable conditions make it possible to determine the magnitude and origin of the anharmonicity.

Motivated by the above considerations, we performed a detailed study of the temperature and pressure dependence of the static dielectric constants and of the Raman-active phonon frequencies in rutile. The purpose of this paper is to present and discuss the results which yield important information concerning the lattice dynamics of this crystal. In Sec. II we review briefly the crystal structure and the nature of the pertinent optic modes. Section III describes the experimental details. The results are presented and discussed in Sec. IV, and finally Sec. V provides an overall summary and conclusions.

II. CRYSTAL STRUCTURE AND OPTICAL PHONONS

Rutile is tetragonal with two TiO_2 molecules per primitive unit cell and belongs to the space group D_{4h}^{14}-$P4/mnm$. The 15 optic modes have the irreducible representations[6,3] $1A_{1g}+1A_{2g}+1A_{2u}+1B_{1g}+1B_{2g}+2B_{1u}+1E_g+3E_u$. Modes of symmetry A_{1g}, B_{1g}, B_{2g}, and E_g are Raman active and modes of symmetry A_{2u} and E_u are infrared active. Figure 1 shows the spatial arrangement of the ions in the unit cell along with the $q \approx 0$ displacements of the Raman-active modes and the A_{2u} mode.

The $A_{2u}(\Gamma_1^-)$ mode is of special interest; it consists of displacements of the positively charged Ti ions against the negatively charged oxygen octahedra in a manner similar to the "Slater" mode in the perovskites. It is the only polar mode with c axis displacements and is the soft FE (TO) mode of the crystal. The temperature and pressure dependence of the soft A_{2u} mode frequency were deduced from dielectric constant data and these dependences were directly measured for the Raman-active modes.

III. EXPERIMENTAL DETAILS

A. Samples

Measurements were made on x-ray-oriented single crystals cut from a good quality boule purchased from the National Lead Co. (South Amboy, N.J.). Chemical analysis showed that the boule was of high purity containing < 10 ppm each of Si, Zr, K, Ag, Ba, Cu, and B and < 1 ppm each of Na, Ca, and Mg. Other elements were sought but not detected within resolution limits of 1–200 ppm. The samples used for the dielectric constant measurements were typically 0.30–0.50 cm^2 in area and 0.06–0.09 cm thick oriented with either the c or a axis perpendicular to the large faces. These faces were vapor coated with aluminum electrodes. The sample used for the Raman scattering measurements was a cube ($\simeq 0.30$ cm^3) cut with the a and c axes perpendicular to the faces.

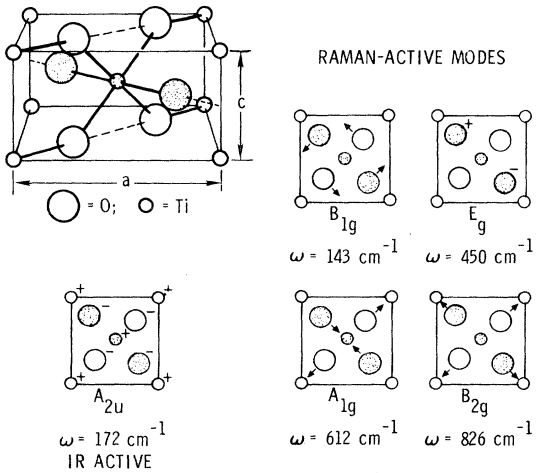

FIG. 1. Rutile structure and $q \simeq 0$ displacements, viewed along the c axis, for the soft A_{2u} mode and Raman active modes.

B. Dielectric Measurements

The dielectric constants were determined from capacitance measurements (to ± 0.2%) performed at 100 kHz using a General Radio model No. 1615-A capacitance bridge. It is known that the static dielectric constants of rutile, especially ϵ_c, exhibit substantial frequency dependence at low frequency,[1,7] associated with surface effects and the presence of oxygen vacancies. We measured the frequency dependence of ϵ_a and ϵ_c at 295 °K for our crystals. ϵ_a was found to decrease slightly up to 5×10^3 Hz and was frequency independent above that, while ϵ_c showed a large decrease with increasing frequency and became constant at frequencies $\geq 10^5$ Hz. Consequently, all subsequent measurements were carried out at 10^5 Hz as values of ϵ_a and ϵ_c at this frequency represent the true values for the crystal. The crystals were lightly held inside a beryllium copper (Berylco 25 hardened to RC 39-41) cell which also served as the high-pressure cell. Shielded electrical high-pressure feed throughs as described by Hammons[8] were employed. Measurements were made either at constant temperature or at heating or cooling rates < 0.2 °K/min. Temperature changes were measured (to ± 0.1 °K) using Cu-constantan thermocouples down to ~30 °K and Cu-AuFe thermocouples (to ± 0.1 °K) at lower temperatures. The temperature dependences of ϵ_a and ϵ_c were measured at 1 bar over the range 4–300 °K and the pressure dependences were measured up to 4.2 kbar at a number of temperatures between 4 and 295 °K using helium (He) gas as the pressure transmitting fluid. Since He solidifies at high pressure at 4 °K, the pressure was applied at high temperature, where the He was gaseous. The cell was then cooled to 4 °K at essentially constant volume and the pressure decrease with decreasing temperature in the solid phase was corrected to constant pressure using Dugdale's[9] He isochore data. The system used to compress the He gas is similar to that described by Schirber.[10]

C. Raman Measurements

The Raman spectra were obtained with an argon laser operating at 4880 Å with incident power ~100 mW. The sample was a polished single crystal with faces normal to the c and a axes. Light scattered at 90° to the incident beam was analyzed with a double-grating spectrometer and detected with a cooled photomultiplier (PM). Signals from the PM were measured using photon counting elec-

tronics and the output was plotted on a recorder.

To obtain the temperature variation of the Raman-active modes, the sample was mounted in a variable temperature Dewar and cooled with the boil off from liquid helium for $T < 295$ °K. The temperature was stabilized to ±0.1 °K and monitored at the sample block using either Ge or Pt resistance thermometers. For $T > 295$ °K the sample was mounted in an oven and the temperature was measured with a thermocouple.

The hydrostatic optical pressure cell used in these experiments was similar to that used by Brafman *et al.*[11] It was made of nickel maraging steel and had three optic windows of fused silica to allow a 90° scattering geometry. The pressure fluid was Isopar H (Humble Oil Co.). Pressure was measured to ±20 psi with a Heise Bourdon tube gauge calibrated against a dead-weight gauge.

D. Compressibility and Thermal Expansions

In calculating the dielectric constants (ϵ) from the measured capacitances (C) at different pressures and temperatures it is necessary to take into account changes in sample dimensions due to compression and thermal expansion. Recall that $\epsilon = Ct/\epsilon_0 A$, where t is the thickness of the sample, A is its area, and $\epsilon_0 = 8.85\times10^{-12}$ F/m is the permittivity of free space. The dimensional corrections for an anisotropic crystal such as rutile are easily made if the axial compressibilities and thermal expansivities are known. The compressibility and thermal expansion are of added importance to us since they enter into much of the analysis and discussion in the rest of the paper.

The effects of temperature from 4 to 1300 °K on the lattice parameters a and c of rutile have been measured by Mauer and Bolz of the U. S. National Bureau of Standards using powder x-ray-diffraction techniques. The data were kindly made available to us by Mauer. Representative values of the lattice parameters a (c) in Å are 4.5869(2.9536), 4.5875(2.9538), 4.5888(2.9551), and 4.5931(2.9586) at 4.2, 77.3, 150, and 298 °K, respectively. Values of the volume expansion coefficient $\beta \equiv (\partial \ln V/\partial T)_P$ calculated from the data will be presented in Sec. IV (see Table II). The thermal expansion of rutile has also been reported by Kirby[12] from 100 to 700 °K using an interferometric technique. There is good agreement between the two measurements.

The axial compressibilities were calculated from the 298 °K elastic constants reported by Manghnani.[4] For a tetragonal lattice the necessary constants are c_{11}, c_{12}, c_{13}, and c_{33}. The compressibilities are then calculated by standard formulas.[13] The elastic constants of course yield the adiabatic compressibilities, but the small differences between these and the needed isothermal compressibilities are insignificant for our purposes. The calculated compressibilities are $\kappa_a \equiv -(\partial \ln a/\partial P)_T = 1.93\times10^{-4}$ kbar^{-1} and $\kappa_c \equiv -(\partial \ln c/\partial P)_T = 0.87\times10^{-4}$ kbar^{-1}. The volume compressibility is then simply $\kappa \equiv -(\partial \ln V/\partial P)_T = 2\kappa_a + \kappa_c = 4.73\times10^{-4}$ kbar^{-1}, a relatively small value. Manghnani also measured the elastic constants at several temperatures up to 373 °K. His results show that κ increases by ~1.8% between 298 and 373 °K. For our purposes we need the κ's at low temperatures. In the absence of low-temperature elastic constant data we assume that κ varies linearly with temperature over the range of interest and with the slope indicated above. On this basis we estimate a decrease in κ of ~7% between 298 and 4 °K. This should be a good estimate, and one can easily show that even substantial uncertainties in it do not significantly affect our conclusions.

IV. RESULTS AND DISCUSSION

A. Dielectric Constants

1. Temperature and Pressure Effects

Figure 2 shows the variation of the reciprocal dielectric constants with temperature at 1 bar. The crystal is quite anisotropic with ϵ_c increasing from 166.7 at 296 °K to 251 at 4 °K, while ϵ_a increases from 89.8 to 114.9 over the same range. These values are slightly different from those reported by Parker[1] but the differences can be accounted for on the basis of the fact that the orientation of our c sample was 0.8° off axis, and that of the a sample was 1.5° off axis. Otherwise the agreement with Parker's results is excellent.

The data can be very well fitted over the whole temperature range by the modified Curie–Weiss law

$$\epsilon = A + \frac{C}{\frac{1}{2}T_1 \coth(T_1/2T) - T_0}, \tag{1}$$

which was first derived (with $A = 0$) by Barrett[14] to describe the deviations from the simple Curie–Weiss behavior in the perovskites at low temperatures. In this equation A, C, T_1, and T_0 are constants at any given pressure. We shall comment on their values and pressure dependences, as well as on the validity of Eq. (1), later. The equation reduces to $\epsilon = A + C/(\frac{1}{2}T_1 - T_0) \equiv$ const as $T \to 0$ and to $\epsilon = A + C/(T - T_0)$ at high temperatures. The solid lines in Fig. 2 represent least-squares fits of the data to Eq. (1). Values of the parameters are shown in Table I. The dashed lines in Fig. 2 indicate the T range over which a simple Curie–Weiss law $\epsilon = C/(T - T_0)$ is approximately valid. We note that values of C and T_0 determined from these dashed lines, namely, $C = 1.2\times10^5$ °K and $T_0 = -430$ °K for the c axis and $C = 9.6\times10^4$ °K and $T_0 = -790$ °K for the a axis, are considerably different from those determined from Eq. (1) (see

TABLE I. Values of the parameters A, C, T_1, and T_0 and some of their logarithmic pressure derivatives for rutile. The parameters were determined from least-squares fits of the static dielectric constants ϵ_c (T) and ϵ_a (T) data to Eq. (1). Similar data for $KTaO_3$ are listed for comparison.

		A	C (10^4 °K)	$\frac{d\ln C}{dP}$ (% kbar^{-1})	T_1 (°K)	$\frac{dT_1}{dP}$ (°K kbar^{-1})	T_0 (°K)	$\frac{dT_0}{dP}$ (°K kbar^{-1})
TiO_2	(c axis)	81.7	3.95	−0.5	135.4	2.0	−165.9	−1.9
			(12.0)[a]				−(430)[a]	
	(a axis)	60.9	1.39	...	156.8	...	−178.9	
			(9.6)[a]				−(790)[a]	
$KTaO_3$[b]		48.3	5.52	−0.8	53.3	1.9	11.8	−4.6

[a]Values determined from the dashed lines in Fig. 2 based on a simple Curie–Weiss law for $\epsilon(T)$.
[b]Values determined by Abel (Ref. 16).

Table I).

Figure 3 shows the pressure dependences of ϵ_a and ϵ_c at various temperatures. The decreases are linear over the 4-kbar range of the measurements.

Values of ϵ_a, ϵ_c, and their temperature and pressure derivatives at different temperatures are summarized in Table II. These values have been corrected for the small dimensional changes of the samples due to volume expansion and compression.

The combination of the temperature and pressure data presented above allow us to use Eq. (1) to evaluate the pressure derivatives of the quantities C, T_1, and T_0. Following the procedure recently outlined by Abel[15] [his Eqs. (3)–(5)] we obtained the values summarized in Table I. For comparison the table also gives the corresponding values for the incipient ferroelectric $KTaO_3$ as determined by Abel. Note that the pressure derivatives are quite comparable in both sign and magnitude for the two crystals.

The parameter A is the T-independent contribution to the polarizability (or ϵ) and was found for

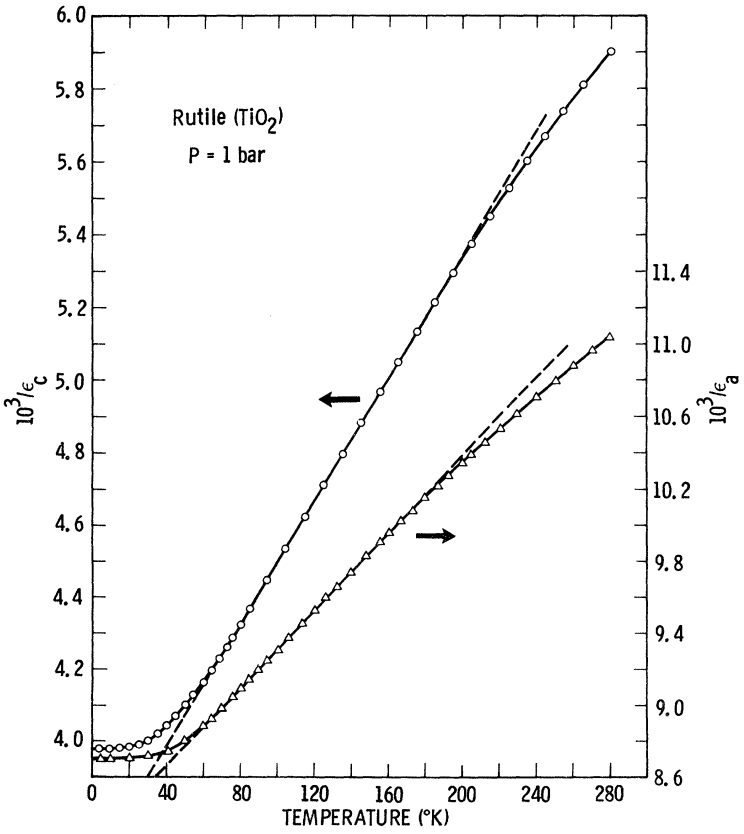

FIG. 2. Temperature dependences of the reciprocal static dielectric constants along the a and c axes. The solid lines are fits of the data to Eq. (1), whereas the dashed lines depict the range where the simple Curie–Weiss law is approximately valid.

TABLE II. Values of the static dielectric constants (ϵ) of rutile and their logarithmic pressure and temperature derivatives. Also listed are the volume thermal-expansion coefficient (β) and volume compressibility (κ). The measured isobaric temperature derivatives are separated into their pure-volume and pure-temperature contributions.

T (°K)		ϵ	β (10^{-5} °K^{-1})	κ (10^{-4} kbar^{-1})	$\left(\frac{\partial \ln\epsilon}{\partial P}\right)_T$ (10^{-3} kbar^{-1})	$\left(\frac{\partial \ln\epsilon}{\partial T}\right)_P$ (10^{-4} °K^{-1})	$= -\frac{\beta}{\kappa}\left(\frac{\partial \ln\epsilon}{\partial P}\right)_T$ (10^{-4} °K^{-1})	$+ \left(\frac{\partial \ln\epsilon}{\partial T}\right)_V$ (10^{-4} °K^{-1})
4.0	c axis	251.0	~0	4.40	-11.8 ± 0.3	~0	~0	~0
	a axis	114.9			-5.18 ± 0.10	~0	~0	~0
75.6	c axis	233.6	0.96	4.48	-11.7 ± 0.1	-18.6 ± 0.4	2.5	-21.1
	a axis	110.6			-5.14 ± 0.07	-11.6 ± 0.3	1.1	-12.7
165.0	c axis	197.9	1.68	4.58	-9.1 ± 0.1	-16.3 ± 0.3	3.4	-19.7
250.0	c axis	175.2	2.14	4.68	-7.6 ± 0.1	-12.0 ± 0.3	3.5	-15.5
296.0	c axis	166.7	2.35	4.73	-7.2 ± 0.1	-9.9 ± 0.3	3.5	-13.4
	a axis	89.8			-3.47 ± 0.04	-6.5 ± 0.2	1.8	-8.3

$KTaO_3$ to be independent of pressure within experimental error.[15] It presumably represents contributions to ϵ from the electronic polarizabilities and lattice modes other than the soft FE mode. Its value is quite large and substantially higher for rutile than for $KTaO_3$. The reason for this is not completely understood, but an important consideration must be the fact that in rutile some of

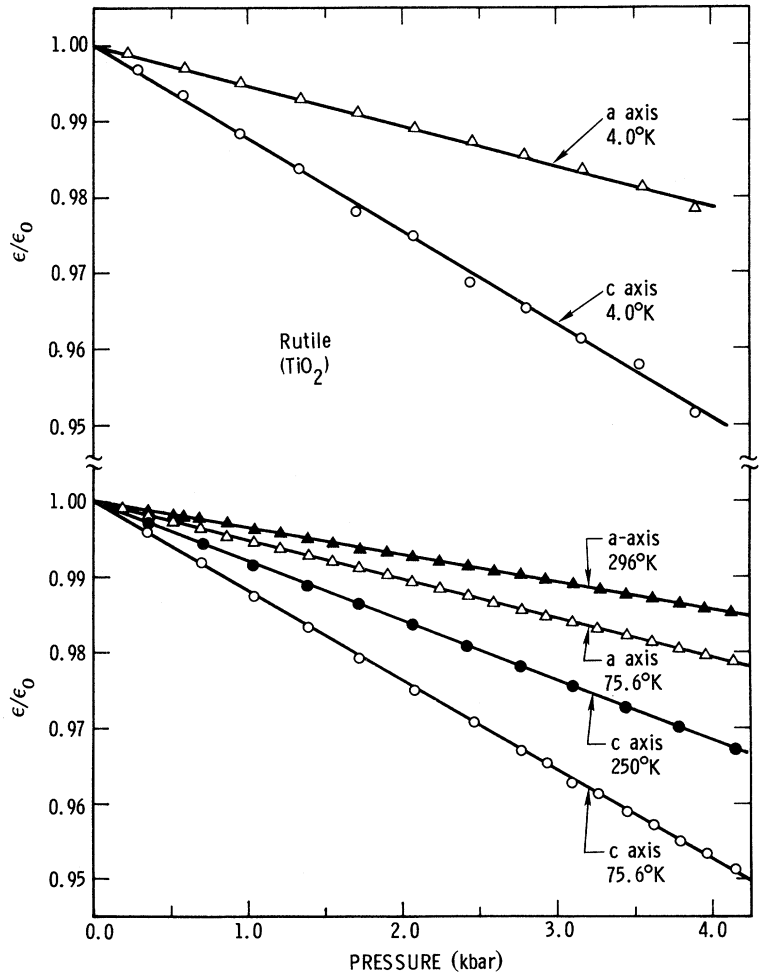

FIG. 3. Isothermal pressure dependence of ϵ_a and ϵ_c at various temperatures.

the oxygen-oxygen distances are smaller than usual.[16] Thus, nonpolar optic vibrations of the crystal may lead to large electronic deformations and hence large contributions to the ionic polarizability, despite the fact that (along the c axis for example) only the FE mode is polar. Such effects add an extra contribution to ϵ. That this is indeed likely to be the case is evidenced by the fact that rutile exhibits much larger second-order Raman scattering intensity than do many other crystals having the rutile structure. This has been noted in the literature[3] and was evident in our Raman studies of rutile.

The pressure dependence of the parameters C, T_1, and T_0 in Eq. (1) can be qualitatively understood in the following way. Equation (1), with $A=0$, was derived by Barrett[14] to account for the deviation of ϵ from a simple Curie–Weiss law at low temperatures observed for several perovskites with low Curie–Weiss temperatures (T_0), e.g., $KTaO_3$ and $SrTiO_3$. The crystal is treated as a system of independent ions in anharmonic potential wells, and the ionic polarizabilities were treated quantum mechanically. The ground state of the ion has energy equal to kT_1, so that for $T < T_1$ all ions are in their lowest energy states and lowering T further causes no change in polarizability or ϵ. Thus, one can view T_1 as the temperature below which deviation from the *simple* Curie–Weiss law occurs. An examination of the dashed lines in Fig. 2 suggests that T_1 should be ~70 °K; however, the best fits of the data to Eq. (1) (solid lines) yield values of T_1 nearly twice this large (see Table I). This results from the fact that A has a relatively large value. The increase in T_1 with pressure is to be expected if in fact T_1 is related to the ground-state energy of the ion. Reducing the interionic separation raises the ground-state energy and hence T_1.[15]

Barrett expressed C and T_0 in terms of constants appearing in the anharmonic potential, but they could not be evaluated from first principles, and are therefore treated as empirically determined parameters. The pressure derivatives of C and T_0 for rutile (Table I) are quite comparable to those observed for many perovskites. The decrease of T_0 with pressure is associated with an increase in the frequency of the soft FE mode (see discussion below) and the decrease in C can also be qualitatively rationalized in terms of the pressure dependences of the polarization and soft mode parameters as discussed elsewhere.[17]

The Barrett treatment suffers a difficulty in attempting to treat experimental results quantitatively. As was first pointed out by Abel,[15] the theory predicts a relationship between the pressure derivatives of C, T_1, and T_0 [Abel's Eq. (7)] which was not consistent with measurements on $KTaO_3$. The same difficulty is encountered in treating the present rutile results.

Finally, we note that the qualitative features of the pressure and temperature dependences of the dielectric constants discussed above, and in particular the increase in T_1 with pressure, were recently treated from a completely different point of view by Gillis.[18] We shall comment briefly on his results in Sec. IV B.

2. *Explicit Volume and Temperature Dependence of ϵ*

The measured temperature dependence of the dielectric constant at constant pressure arises from two contributions[19]: (i) the change which arises solely from the change in lattice spacings or density, i.e., the explicit volume effect and (ii) the explicit temperature dependence which would occur even if the volume of the sample were to remain fixed. Writing $\epsilon = \epsilon(V, T)$ we then have

$$\left(\frac{\partial \ln\epsilon}{\partial T}\right)_P = \left(\frac{\partial \ln V}{\partial T}\right)_P \left(\frac{\partial \ln\epsilon}{\partial \ln V}\right)_T + \left(\frac{\partial \ln\epsilon}{\partial T}\right)_V$$

$$= -\frac{\beta}{\kappa}\left(\frac{\partial \ln\epsilon}{\partial P}\right)_T + \left(\frac{\partial \ln\epsilon}{\partial T}\right)_V , \tag{2a}$$

where $\beta \equiv (\partial \ln V/\partial T)_P$ is the volume thermal-expansion coefficient and $\kappa \equiv -(\partial \ln V/\partial P)_T$ is the isothermal volume compressibility. Thus the constant volume contribution can be evaluated from the measured isobaric and isothermal derivatives and a knowledge of β and κ. Table II summarizes the results for the two crystallographic orientations. It is clear from these results that the pure-volume and pure-temperature contributions are opposite in sign and that the pure-temperature effect $(\partial \ln\epsilon/\partial T)_V$ is by far the predominant term in determining the isobaric temperature dependence of ϵ. This is unlike the behavior of normal ionic crystals such as the alkali halides where $(\partial \ln\epsilon/\partial T)_V$ is very small and the pure-volume contribution dominates. That the pure-temperature effect dominates in rutile is of course expected since both ϵ_a and ϵ_c decrease with pressure and also exhibit large and anomalous decreases with increasing T. The results in Table II just make this fact more quantitative.

The above conclusion is made more explicit by evaluating the pure volume and pure temperature changes in ϵ over the whole temperature range covered by the measurements. To do so we rewrite Eq. (2a) in the form

$$(\Delta\epsilon_T)_P = -(\Delta\epsilon_P)_T + (\Delta\epsilon_T)_V . \tag{2b}$$

In this notation $(\Delta\epsilon_T)_P$ is the measured change in ϵ on raising the temperature from 0 to T °K at constant pressure (1 bar); $(\Delta\epsilon_T)_V$ is the change in ϵ caused by raising the temperature from 0 to

T °K at constant volume, that being the volume of the crystal at 0 °K and 1 bar; $-(\Delta\epsilon_P)_T$ is the change in ϵ caused by raising the pressure at constant temperature T from 1 bar to a value P sufficient to produce a volume change equal in magnitude to that caused by raising the temperature from 0 to T °K at 1 bar. It is readily evaluated from $\epsilon(P)$ data and the known compressibility and thermal expansion. Obviously, this term enters with a negative sign [Eq. (2a)] since the signs of the compressibility and thermal expansion of rutile are normal, i.e., ΔV is positive on heating and negative on compression. The experimental $\epsilon(T, P)$ data yield the results in Fig. 4. These results clearly show the dominance of the pure temperature effect at all temperatures in determining the isobaric $\epsilon(T)$ dependences of both ϵ_a and ϵ_c.

The above results for rutile are very similar to those obtained for many paraelectric perovskites and incipient ferroelectrics. For such materials it is customary to discuss the temperature dependence of ϵ in terms of either (i) a "near" polarization catastrophe,[1] whereby on lowering the temperature the polarization fluctuations become large and the local fields increase faster than the elastic restoring forces or (ii) a "soft" TO phonon whose frequency decreases with decreasing temperature. These two approaches are, in fact, two different ways of saying the same thing, and they are related via the Lyddane–Sachs–Teller (LST) relation.[20]

In terms of the polarization catastrophe, the static and high-frequency (ϵ_∞) dielectric constants are related via the local fields at the various lattice sites to either macroscopic or to microscopic polarizabilities of the individual ions.[1,21] Using the resulting generalized Clausius–Mossotti relationship, measurements of the pressure and temperature dependences of the dielectric constants can be combined to evaluate the explicit volume and temperature dependences of the polarizabilities.

The pressure and temperature dependences of the ϵ_∞'s of rutile are known and are much smaller than those of the static constants[22]: The logarithmic pressure derivatives at 295 °K are 8.5×10^{-5} kbar^{-1} and -34×10^{-5} kbar^{-1} and the logarithmic temperature derivatives at 1 bar are $\sim-3.5\times10^{-5}$ °K^{-1} and $\sim-5.3\times10^{-5}$ °K^{-1} for $\epsilon_{\infty,a}$ and $\epsilon_{\infty,c}$, respectively.

Making use of this and following earlier procedures,[21] we find that it is the explicit T dependence of the lattice (or infrared) polarizability α_{ir}, i.e., $(\partial\alpha_{ir}/\partial T)_V$, which makes the dominant contribution to the T dependence of the static dielectric constants at constant pressure. This explicit T dependence of α_{ir} arises from anharmonic terms in the crystal potential and relates directly to the T dependence of the phonon frequencies, hence the question of "soft" TO phonons which will be discussed below.

B. Relationship between ϵ and the Soft-Mode Frequency

It has been shown[20,23,5] that for a uniaxial crystal such as rutile, the generalized LST relationship can be written (for the c axis)

$$\frac{\epsilon_c}{\epsilon_{\infty,c}}=\prod_i\left(\frac{\omega_{c,\mathrm{LO}}}{\omega_{c,\mathrm{TO}}}\right)_i^2 \qquad (q\simeq 0)\ , \tag{3}$$

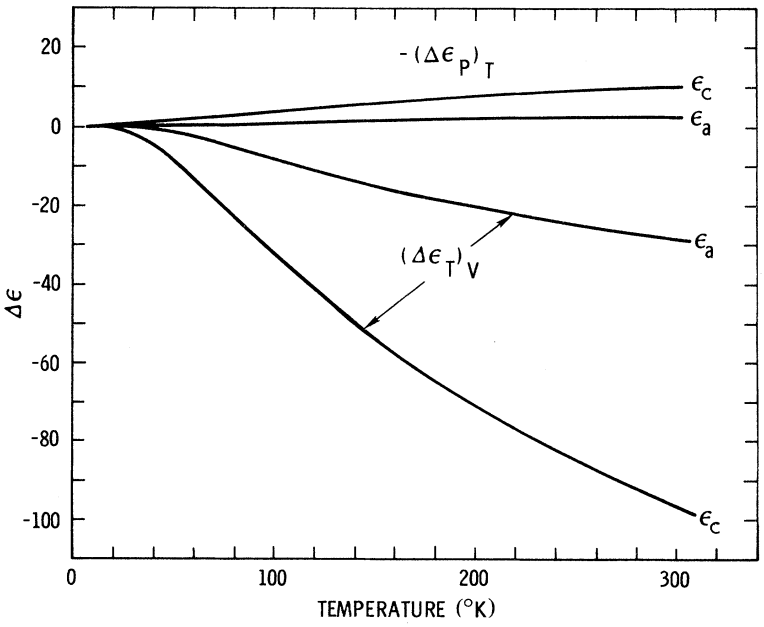

FIG. 4. Changes in the static dielectric constants ϵ_a and ϵ_c of rutile due to the pure-volume $-(\Delta\epsilon_P)_T$ and pure-temperature $(\Delta\epsilon_T)_V$ effects.

with a similar expression for the a axis. Here ω_{LO} and ω_{TO} are the long-wavelength ($q \approx 0$) longitudinal- and transverse-optic phonon frequencies. The product is taken over all of the optic modes i. As mentioned earlier (Sec. II) rutile has only one pair of LO-TO polar modes with displacements along the c axis, namely, the FE mode of symmetry A_{2u}. The c axis expression then reduces to the simple form

$$\frac{\epsilon_c}{\epsilon_{\infty,c}} = \left(\frac{\omega_{c,LO}}{\omega_{c,TO}}\right)^2_{A_{2u}} . \tag{4}$$

As is generally true, ϵ_∞ and ω^2_{LO} should be nearly independent of temperature and the large temperature dependence of ϵ_c should be associated with that of $\omega_{TO} (\equiv \omega_f$, where the subscript f indicates the FE mode) in such a manner that

$$\epsilon_c \omega_f^2 = \text{const.} \tag{5}$$

That the large increase in ϵ_c on cooling is almost completely due to a decrease in ω_f according to Eq. (5) is shown in Fig. 5 where we plot ω_f^2 vs T. The data points represent the recent results of Traylor *et al.*[5] determined directly from inelastic neutron scattering measurements. The solid line is deduced from our $\epsilon_c(T)$ data and the use of Eq. (5), where the constant was evaluated from the known room-temperature (300 °K) values of $\epsilon_c = 166.2$ and $\omega_f = 172$ cm^{-1}. Within the $\pm 1\%$ uncertainty of the neutron-determined frequencies the agreement between the two results is quite good. We note briefly that unlike $SrTiO_3$, where $\omega_f^2(T)$ is linear over a relatively large T range above ~50 °K, rutile exhibits a large deviation from linearity at high temperature, and in this respect it resembles more closely $KTaO_3$.[24,25] This is of course also manifested by the fact that $\epsilon_c(T)$ does not obey a simple Curie–Weiss law. We shall come back to a discussion of the $\omega_f(T)$ dependence later.

TABLE III. Values of the soft-mode frequency ω_f and the logarithmic pressure derivatives of ω_f and the c-axis static dielectric constant ϵ_c of rutile at different temperatures.

T (°K)	ω_f[a] (cm^{-1})	$\left(\frac{\partial \ln \epsilon_c}{\partial P}\right)_T$ (% kbar^{-1})	$\left(\frac{\partial \ln \omega_f}{\partial P}\right)_T$ (% kbar^{-1})
4	142	−1.18	0.59
75.6	148	−1.17	0.58
165	159	−0.91	0.45
250	168	−0.76	0.38
300	172	−0.72	0.36

[a]Values taken from Ref. 5.

From the above considerations it is seen that measurements of ϵ_c give us essentially direct information on ω_f. We make use of this fact in deducing the effect of pressure on ω_f from the $\epsilon_c(P)$ data. This was necessary because the A_{2u} mode is not Raman active and we could not measure $\omega_f(P)$ directly. From Eq. (5) it follows that

$$\left(\frac{\partial \ln \omega_f}{\partial P}\right)_T = -\tfrac{1}{2}\left(\frac{\partial \ln \epsilon_c}{\partial P}\right)_T . \tag{6}$$

Table III gives values of these two quantities as well as ω_f at different temperatures.

The increase in ω_f with pressure is to be expected. An examination of the displacements associated with this soft mode (Fig. 1) suggests that ω_f should increase as we decrease the interionic distances. As in the case of the perovskites,[26]

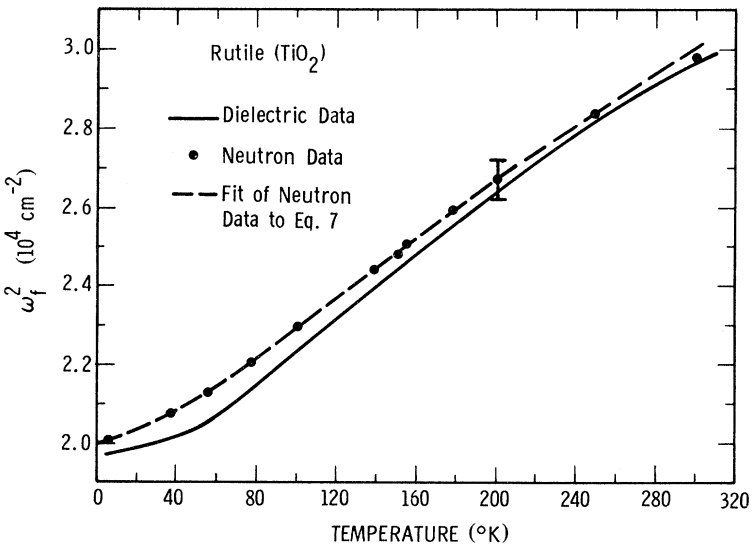

FIG. 5. Comparison of the temperature dependence of the soft-mode frequency squared from neutron scattering and dielectric constant measurements. The dashed curve represents a fit of the neutron data to Eq. (7).

the magnitude of the increase is relatively large considering the fact that the increase in crystal density is only $\simeq 0.05\%\,\text{kbar}^{-1}$ for rutile. This feature and the increase in $\partial \ln\omega_f/\partial P$ with decreasing temperature are manifestations of the unique properties of the FE mode. The frequency ω_f of this mode is determined by a balance between short-range and Coulomb forces. The short-range forces increase more rapidly with increasing pressure than do the Coulomb forces, and thus a small variation in crystal volume leads to a relatively large change in ω_f, and this effect becomes fractionally larger as ω_f becomes smaller.[26]

The pressure and temperature dependences of ω_f and ϵ of rutile can also be qualitatively treated in a manner similar to that recently employed by Gillis.[18] Using a model paraelectric crystal with nearest-neighbor anharmonic short-range interaction and a harmonic dipolar interaction and employing a self-consistent renormalization procedure for the frequency spectrum, he was able to qualitatively reproduce the increase in ω_f and T_1 with pressure observed for $KTaO_3$.[15] His results should be equally applicable for rutile. The increase in ω_f with pressure can be understood on physical arguments similar to those advanced in the above paragraph. The increase in T_1, on the other hand, can be understood by observing that the theory shows that the degree to which the linear temperature dependence of ω_f^2 extends into the low-temperature regime is strongly dependent on the density of occupied $q \approx 0$ soft modes with $\hbar\omega/kT < 1$. The density of such modes decreases with increasing pressure leading to an increase in T_1 (see Sec. IV A).

Finally, we comment that the excellent fit of the $\epsilon(T)$ data to the Barrett expression [Eq. (1)] indicates that the $\omega_f(T)$ data can also be well fitted by a similar expression appropriately related to Eq. (1). However, in view of the question raised earlier as to the interpretation of Eq. (1), which is based on an anharmonic oscillator model, it is worth noting that the $\omega_f(T)$ data can be very well fit by the quasiharmonic model expression

$$\omega_f^2 = \omega_0^2 + \int \rho(\omega) n(\omega, T)\, d\omega = \omega_0^2 + B(e^{\theta_E/T} - 1)^{-1} \tag{7}$$

suggested by Worlock.[27] Here ω_0 is the value of ω_f at 0 °K, $\rho(\omega)$ is a density function which accounts for the anharmonic interactions (related to Δ defined later), and $n(\omega, T)$ is the phonon occupation number. The second equality in Eq. (7) follows from assuming an Einstein spectrum for $\rho(\omega)$. The dashed line in Fig. 5 is a fit to the neutron data with $B = 1788$ and $\theta_E = 48.9$ °K. Unfortunately, the fit is not unique as B and θ_E are highly correlated, and the physical significance of the fit remains uncertain—a circumstance also emphasized by Worlock.

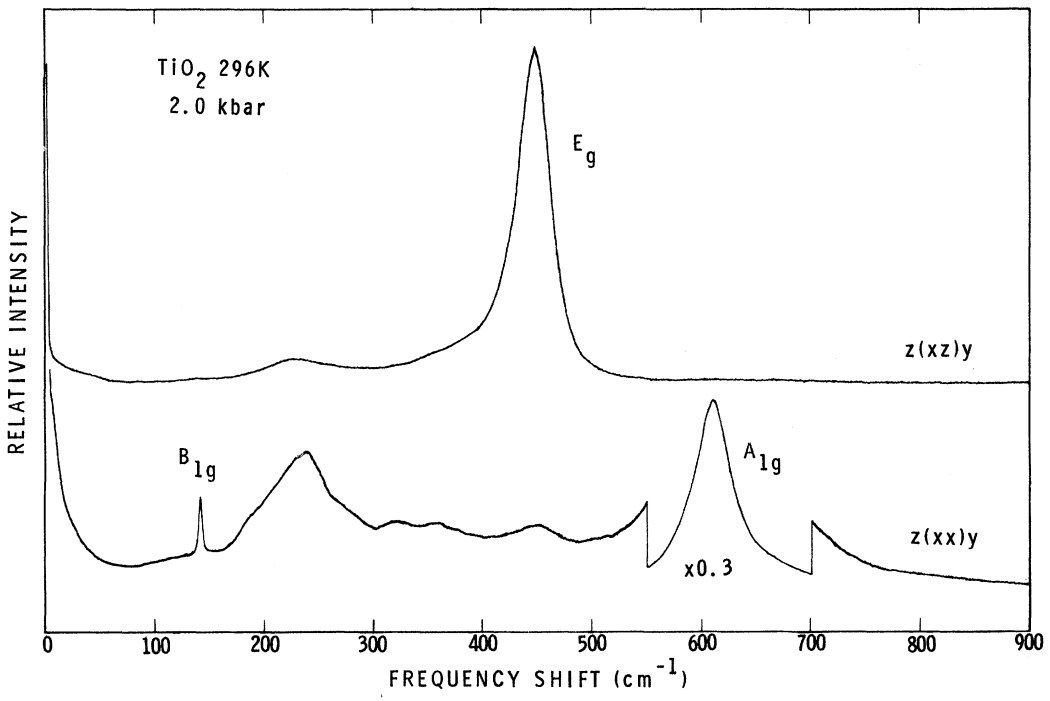

FIG. 6. Raman spectra taken at 2.0 kbar and 296 °K showing modes of symmetry A_{1g}, B_{1g} $[z(xx)y]$, and E_g $[z(xz)y]$.

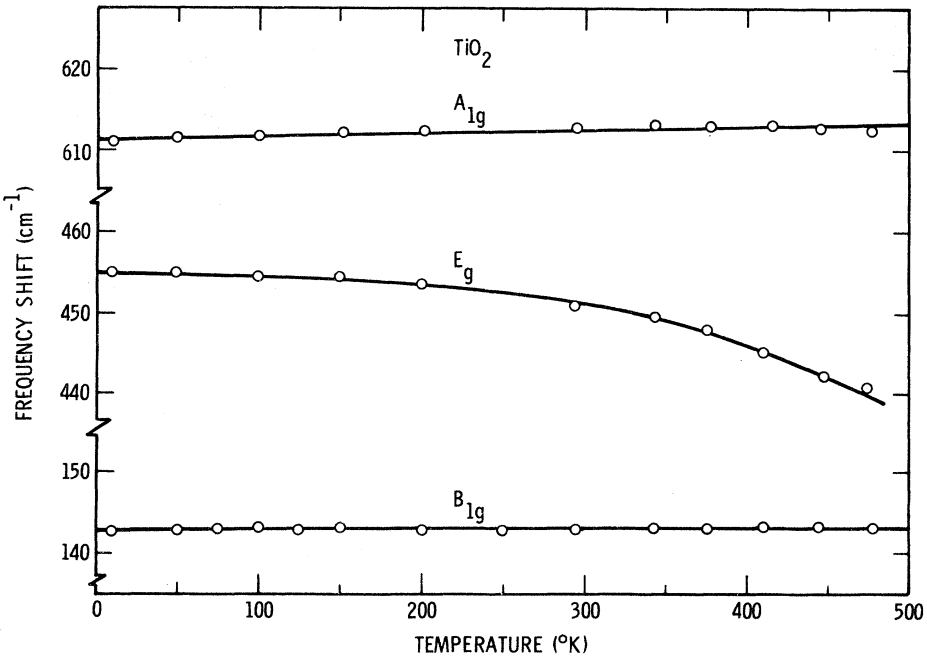

FIG. 7. Temperature dependences of the frequencies of the Raman-active modes A_{1g}, E_g, and B_{1g} measured at 1 bar.

C. Raman-Active Phonons

1. Effects of Temperature and Pressure

Typical Raman spectra for different scattering geometries obtained in the pressure cell are shown in Fig. 6. The spectra show clear evidence for strong second-order scattering. The measured shifts of the phonon frequencies with temperature and pressure are given in Figs. 7 and 8 and Table IV. The table also includes the corresponding values for the soft A_{2u} mode for completeness. Our values of the frequencies at 1 bar and 296 °K are in good agreement with those of Porto *et al.*[3] The temperature dependences of the Raman fre-

TABLE IV. Values of the frequencies (ω) of some of the optic phonons of rutile and their logarithmic pressure and temperature derivatives and mode Grüneisen parameters (γ). The measured isobaric temperature derivatives are separated into their pure-volume and pure-temperature contributions.

	T (°K)	ω (cm^{-1})	$\left(\frac{\partial \ln\omega}{\partial P}\right)_T$ (10^{-3} kbar)$^{-1}$)	γ	$\left(\frac{\partial \ln\omega}{\partial T}\right)_P$ (10^{-5} °K^{-1})	$= -\frac{\beta}{\kappa}\left(\frac{\partial \ln\omega}{\partial P}\right)_T$ (10^{-5} °K^{-1})	$+ \left(\frac{\partial \ln\omega}{\partial T}\right)_V$ (10^{-5} °K^{-1})
B_{1g}	296	143	-2.38 ± 0.2 $-(2.1)$ [a]	-5.03	0.60 ± 0.4	11.82	11.22
E_g	296	450	1.15 ± 0.2 (1.0) [a]	2.43	-6.30 ± 0.4	-5.71	-0.59
A_{1g}	296	612	0.75 ± 0.2 (0.67) [a]	1.59	0.60 ± 0.4	-3.72	4.32
B_{2g}	296	826 [b]					
A_{2u}	296	172	3.6 ± 0.1	7.61	49.5 ± 1.5	-17.9	67.4
A_{2u}	250	168	3.8 ± 0.1	8.12	60.0 ± 1.5	-17.3	77.3
A_{2u}	165	159	4.5 ± 0.1	9.82	81.5 ± 1.5	-16.4	97.9
A_{2u}	75.6	148	5.8 ± 0.1	12.95	93.0 ± 2.0	-12.4	105.4
A_{2u}	4	142	5.9 ± 0.15	13.32	~ 0	~ 0	~ 0

[a] Values reported by Nicol and Fong (Ref. 28).

[b] This mode was not well resolved and exhibited such small shifts that accurate measurements of the pressure and temperature dependences could not be made.

quencies apparently have not been reported earlier. Our pressure derivatives of these frequencies are in agreement with the recent results of Nicol and Fong[28] (see Table IV). Our data are more accurate than theirs because of the presence of some pressure gradients and uncertainty in the value of the pressure in their apparatus; however, these effects appear compensated for by their ability to cover a larger range of pressure.

Although the Raman modes in general exhibit relatively weak pressure and temperature shifts compared with A_{2u}, the results in Figs. 7 and 8 and Table IV contain a number of interesting features worthy of comment. In addition to A_{2u}, the modes B_{1g} and A_{1g} exhibit anomalous T dependences in that their ω's increase with increasing T, though the changes are very small. Mode B_{1g} is especially anomalous in that unlike all of the other modes its frequency *decreases* with increasing pressure. We shall comment on this later. Mode E_g is the only mode studied which exhibits the kind of behavior usually expected in "normal" ionic crystals, namely, $\omega(E_g)$ increases with increasing pressure and decreases with increasing temperature. The scattering intensity of the B_{2g} phonon is relatively weak and its temperature and pressure shifts so small that they could not be measured accurately.

It is quite instructive to examine the isobaric temperature derivatives of the frequencies in terms of their pure-volume and pure-temperature contributions. Following the procedure used in Sec. IV A to examine the $\epsilon(T,P)$ results [see Eq. (2)], we obtain the results summarized in Table IV and evaluated at 296 °K.[19] As expected, for the FE mode A_{2u} the isobaric frequency shift is heavily dominated by the pure temperature contribution $(\partial \ln\omega/\partial T)_V$ which arises from high-order anharmonic interactions, and which is opposite in sign from the pure-volume contribution $-(\beta/\kappa)(\partial \ln\omega/\partial P)_T$. In the case of B_{1g} the pure-volume and pure-temperature contributions are both large and about equal but opposite in sign leading to nearly perfect cancellation, and thus the weak isobaric temperature dependence of $\omega(B_{1g})$. The same is true of A_{1g}, but here the signs of the two contributions are reversed and the pure temperature contribution determines the anomalous positive sign of the isobaric derivative. Mode E_g exhibits "normal" ionic crystal behavior: Its pure temperature contribution is small and the isobaric shift is dominated by the pure volume term.

On of the interesting features of the results in Table IV is the sign of the pure temperature contribution. It is large and positive for A_{2u} and rela-

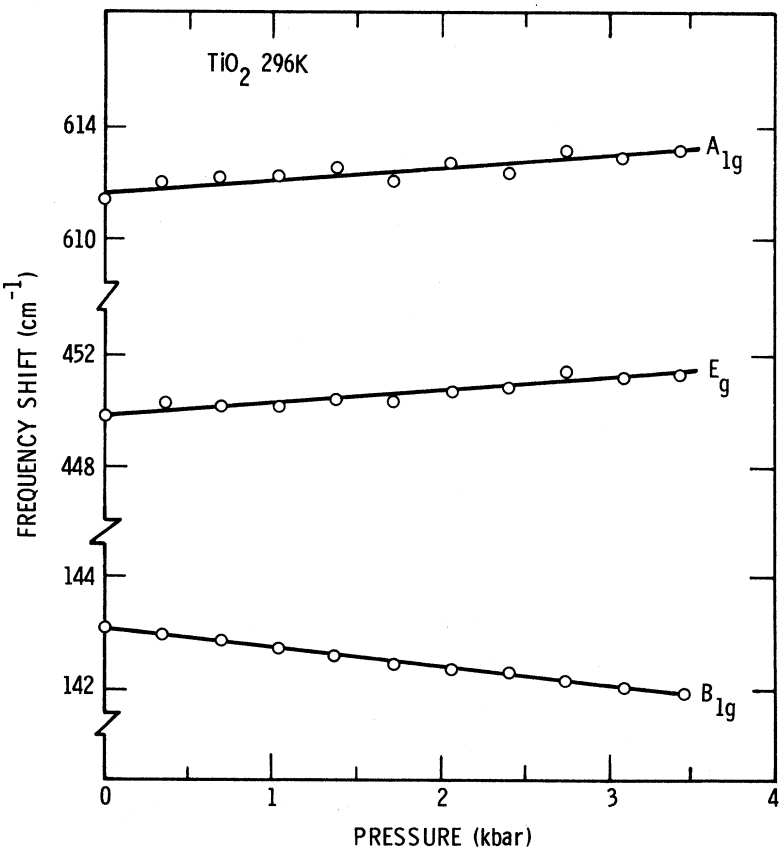

FIG. 8. Pressure dependences of the frequencies of the A_{1g}, E_g, and B_{1g}, Raman-active modes measured at 296 °K.

tively large and negative for B_{1g}. It is also relatively large and positive for A_{1g}. The differences in sign may imply differences in the origin of the anharmonicities for the various modes as will be discussed in Sec. IV D.

2. Mode Grüneisen Parameters

The mode Grüneisen parameters, or so-called mode gammas (γ_i), defined by

$$\gamma_i \equiv -\left(\frac{\partial \ln \omega_i}{\partial \ln V}\right)_T = \kappa^{-1}\left(\frac{\partial \ln \omega_i}{\partial P}\right)_T , \tag{8}$$

can be readily evaluated from the pressure derivatives. Values of the γ_i's at 296 °K for the Raman-active modes and for the soft FE mode at several temperatures are given in Table IV. The values for E_g and A_{1g} are typical for normal ionic crystals. As expected,[26] $\gamma(A_{2u})$ is large and positive and increases with decreasing temperature—properties unique to soft FE modes. For the Raman modes the γ_i's should be very weakly T dependent. The anomalous behavior of B_{1g} is here reflected by its relatively large and negative γ. Some possible consequences of this are discussed in Sec. IV E.

D. Anharmonic Self-Energy of the Optic Phonons

In the above discussion it was shown that for several of the optic modes the isobaric temperature dependence of the phonon frequency is dominated by the volume-independent, or pure-temperature, frequency shift. This shift arises from high-order anharmonicities in the crystal potential. In order to understand its origin we must resort to the lattice dynamical theory of anharmonic crystals. Although detailed treatments of anharmonic lattice dynamics are very complex involving the techniques of many-body theory, there are some approximate models, such as those of Maradudin and Fein[29] and of Cowley,[30] which are useful for our present purposes.

Following Cowley, the renormalized frequency $\omega_T(qj)$ of a mode of wave vector q and branch j can be written

$$\omega_T(qj)^2 = \omega_0(qj)^2 + 2\omega_0(qj)D(qjj',\Omega) , \tag{9}$$

where $\omega_0(qj)$ is the strictly harmonic frequency of the normal mode and $D(qjj',\Omega)$ is the anharmonic contribution to the self-energy of the mode. It depends on the applied frequency Ω whose value can vary depending on the measuring technique; for example $\Omega \simeq 0$ for measuring the static dielectric constant, and $\Omega \simeq \omega_T(qj)$ for measuring neutron scattering properties. The self-energy $D(qjj',\Omega)$ is a complex quantity which can be written

$$D(qjj',\Omega) = \Delta(qjj',\Omega) - i\Gamma(qjj',\Omega) , \tag{10}$$

where the real part Δ measures the anharmonic frequency shift and the imaginary part Γ is the the reciprocal of the phonon relaxation time. The real part of D can be written

$$\Delta(qjj',\Omega) = \Delta^E + \Delta_3 + \Delta_4 + \cdots \equiv \Delta^E + \Delta^A . \tag{11}$$

The contribution Δ^E involves the thermal strain $U^T_{\alpha\beta}$ and represents the anharmonic frequency shift due to thermal expansion. It can be written

$$\Delta^E = \frac{2}{\hbar}\sum_{\alpha\beta} V_{\alpha\beta}(\lambda^-\lambda')U^T_{\alpha\beta} . \tag{12}$$

Of the higher-order anharmonicities, designated by Δ^A, we will explicitly consider only the anharmonic self-energy shift arising from the cubic Δ_3 and quartic Δ_4 terms. These contributions are of the same order, and the leading term from cubic anharmonicity is

$$\Delta_3 = -\frac{18}{\hbar^2}\sum_{\lambda_1}\sum_{\lambda_2}\left|V(\lambda\lambda_1\lambda_2)\right|^2\left(\frac{n_1+n_2+1}{\Omega+\omega_1+\omega_2} - \frac{n_1+n_2+1}{\Omega-\omega_1-\omega_2} + \frac{n_2-n_1}{\Omega+\omega_1-\omega_2} - \frac{n_2-n_1}{\Omega-\omega_1+\omega_2}\right) , \tag{13a}$$

which results from the cubic interaction taken to second order. The first-order term in the quartic interaction yields

$$\Delta_4 = \frac{12}{\hbar}\sum_{\lambda_1} V(\lambda^-\lambda'\lambda_1\lambda_1^-)(2n_1+1) . \tag{13b}$$

In Eqs. (12) and (13), $\lambda_i = (q_i j_i)$, $\lambda^- = (-qj)$, and $\lambda' = (qj')$; $\omega_i = (q_i j_i)$ is the phonon frequency and $n_i = n(q_i j_i) = (e^{\hbar\omega_i/kT} - 1)^{-1}$ is the Bose–Einstein phonon occupation number.

From Eq. (13b) we observe that Δ_4 is frequency (Ω) independent and enters the expression for $\Delta(qjj',\Omega)$ with a positive sign so that its contribution to the anharmonic self-energy can be either positive or negative depending on the sign of the quartic potential. The contribution Δ_3, on the other hand, enters with a negative sign and involves the square of the cubic potential. This term is negative for low values of Ω but can become positive for large Ω. Calculations by Cowley[30] have shown that Δ_3 is negative for the $q \approx 0$ TO modes of $SrTiO_3$ for $\Omega \leq 14\times10^{12}$ sec^{-1} and can become positive for higher frequencies. Thus, under suitable conditions, the sign of the measured higher-order anharmonic frequency shift allows us to deduce the origin of the anharmonicity, assuming that the series for Δ^A converges rapidly. The assumption should be valid in TiO_2, where, as will become clear shortly, the anharmonic contributions to the renormalized frequencies are much less than the harmonic contributions at all temperatures.

We now wish to relate the different contributions in $\Delta(qjj',\Omega)$ to measurable quantities. Δ^E and Δ^A can be separately determined for each measured

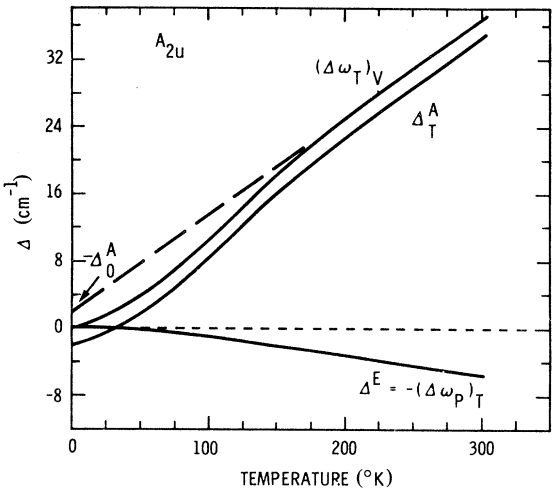

FIG. 9. Pure-volume $-(\Delta\omega_P)_T$ and pure-temperature $(\Delta\omega_T)_V$ contributions to the shift of the soft A_{2u} mode frequency of rutile with temperature.

mode from the pressure and temperature dependences of the phonon frequencies ω. Since $\omega = \omega(V, T)$, we can write, as before,[19]

$$(\Delta\omega_T)_P = -(\Delta\omega_P)_T + (\Delta\omega_T)_V \,, \tag{14}$$

where the Δ's are defined as in Eq. (2b). They are evaluated from the $\omega(T, P)$ data as follows. Our experimental data consist of $\omega(T)$ from $4(\approx 0)$ to 300 °K and $\omega(P)$ at different T's from 4 to 300 °K for the soft FE mode, and $\omega(T)$ from 4 to 500 °K and $\omega(P)$ at 296 °K for the Raman modes. What is lacking is $\omega(P)$ data at different T's for the Raman modes. Considering the small variation and nearly linear $\omega(T)$ and $\omega(P)$ behavior of the Raman modes (see Figs. 7 and 8) and the small compressibility and thermal expansion of rutile, we shall assume that for each mode the Grüneisen parameter γ is independent of T and has its measured 296 °K value given in Table IV. Any small uncertainties introduced by this assumption should not affect our later conclusions. Thus, we have all the information needed to evaluate $(\Delta\omega_T)_V$ and $(\Delta\omega_P)_T$ as functions of T for each of the modes investigated. The results are summarized in Figs. 9 and 10.

The quantities $(\Delta\omega_P)_T$ and $(\Delta\omega_T)_V$ are related to Δ^E and Δ^A, respectively, in Eq. (13) in the following way. Δ^E is simply given by

$$\Delta^E = -(\Delta\omega_P)_T \,. \tag{15}$$

If Δ^A is not too large compared to $\omega_T(qj)$ for a given mode, we can write, following Lowndes,[31]

$$(\Delta\omega_T)_V = \Delta^A \approx \Delta^A_T - \Delta^A_0 \,, \tag{16}$$

where Δ^A is written as shown on the right-hand side to indicate that its value at 0 °K, Δ^A_0, may be different than zero due to anharmonic effects associated with zero-point motion. Since at sufficiently high temperatures the volume and the phonon occupation numbers $n(qj)$ and $(\Delta\omega_T)_V$ are expected to vary linearly in T, an estimate of $-\Delta^A_0$ can be obtained from an extrapolation of the linear $(\Delta\omega_T)_V$ response back to 0 °K. Once this is done, Δ^A_T can be simply determined from $(\Delta\omega_T)_V$. Although our present measurements on rutile extend only to temperatures considerably below the characteristic Debye temperature ($\Theta_D \approx 750$ °K),[5] we still find a nearly linear $(\Delta\omega_T)_V$ response for some of the modes at the high-temperature end of our range (see Figs. 9 and 10), and thus we are able to estimate $-\Delta^A_0$. We note in passing that some considerations of the lattice dynamics of the perovskites[30] similarly indicate high temperature response at temperatures much lower than Θ_D.

We now turn to some observations and conclusions from the results in Figs. 9 and 10. Considering first the FE mode A_{2u} we note that the thermal expansion causes a negative frequency

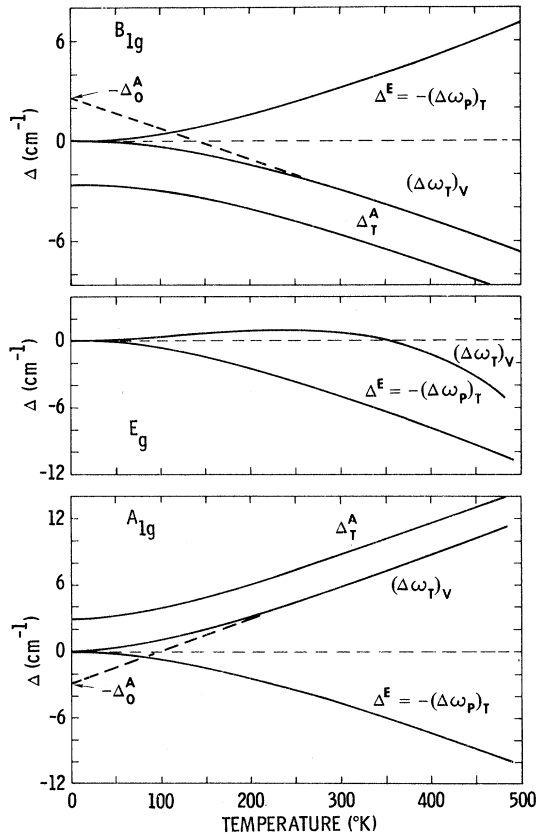

FIG. 10. Pure-volume $-(\Delta\omega_P)_T$ and pure-temperature $(\Delta\omega_T)_V$ contributions to the shift of the frequencies of the B_{1g}, E_g, and A_{1g} Raman-active modes of rutile with temperature.

shift Δ^E amounting to 3.5% of the phonon energy at 300 °K. The volume-independent shift $(\Delta\omega_T)_V$ is large and positive and it is approximately linear in T above ~200 °K making it possible to deduce a value of $-\Delta_0^A$ as shown. Although this value of Δ_0^A (~ -2 cm^{-1}) may be in considerable error because the linear portion of $(\Delta\omega_T)_V$ does not extend over a large T range and because we are at T's substantially below Θ_D, it is clear from the results in the figure that Δ_0^A is relatively small and negative. Using the indicated value of Δ_0^A we deduce the $\Delta_T^A(T)$ dependence shown. This anharmonic self-energy shift is small and negative at low temperatures and becomes large and positive at high temperatures amounting to ~20% of the phonon energy at 300 °K. Since in the approximation discussed above, cubic anharmonicities (Δ_3) lead to a negative Δ^A at low frequencies (Ω), the results in Fig. 9 show that above ~50 °K the self-energy shift of the FE mode is dominated by quartic anharmonicities (Δ_4) and these are positive in sign. It appears that the cubic terms become important below ~50 °K.

It is worth noting here that a similar recent analysis by Lowndes[31] of data on the weak soft-mode crystal TlBr similarly reveal that quartic anharmonicities dominate Δ_T^A in this material. In this crystal, however, Δ_T^A appears to be positive at all temperatures.

For mode B_{1g} the anomalous pressure dependence of the frequency leads to a positive self-energy shift Δ^E due to the thermal expansion (Fig. 10). The figure shows very clearly that Δ^E is counterbalanced at all temperatures by a very nearly equal but negative shift $(\Delta\omega_T)_V$ due to the cubic and quartic anharmonicities, thus accounting for the very weak isobaric T dependence of $\omega(B_{1g})$. As for A_{2u}, Δ_0^A is small (~ -3 cm^{-1}) and negative. The shift Δ_T^A is negative at all temperatures, and in this case it is not possible to say anything about the origin of the anharmonicities. Note that Δ_T^A is much smaller in magnitude here than is the case for A_{2u}.

As we mentioned earlier mode E_g exhibits behavior typical of normal ionic crystals in that the isobaric T dependence of $\omega(E_g)$ is dominated by the thermal expansion term. This is clearly shown in Fig. 10. The pure temperature shift is smaller. Δ_0^A is again negative and Δ_T^A is relatively small and negative at all T, leaving the origin of the anharmonicity ambiguous.

As for B_{1g}, the weak isobaric T dependence of ω for mode A_{1g} is caused by the fact that the shifts due to thermal expansion and higher-order anharmonicities are nearly equal but opposite in sign. The signs of these shifts are, however, opposite from what they are for B_{1g}. Unlike the other modes, the shift Δ_0^A is positive for A_{1g}, and this causes Δ_T^A to be positive at all temperatures. The fact that it is positive suggests that Δ_T^A may be dominated by the quartic anharmonicities in this case.

In the case of the mode B_{2g} the temperature and pressure shifts of $\omega(B_{2g})$ were not determined accurately enough to allow a meaningful separation of the different contributions. However, from the experimental data it was clear that the anharmonic self-energy shifts are small.

In conclusion, the results of this section quantitatively show that for modes E_g, A_{1g}, and B_{2g} the self-energy shifts are small and thus the renormalized mode frequencies ω_T are strongly dominated by the strictly harmonic frequencies ω_0. (This conclusion is not materially affected by the approximations and assumptions made in the data analysis.) The same conclusion is approximately valid for B_{1g}, although here $\omega(B_{1g})$ is small making Δ^E and Δ^A fractionally larger, and furthermore the sign of Δ^E is anomalous. For A_{2u}, of course, the anharmonic self-energy shifts are large and appear dominated by the positive quartic anharmonicities responsible for the soft-mode behavior. The strictly harmonic contribution to $\omega(A_{2u})$ is 144 cm^{-1}, while the total anharmonic contribution to the renormalized frequency is ~28 cm^{-1} at room temperature. The anomalous positive isobaric temperature derivatives of ω_T for modes A_{2u}, B_{1g}, and A_{1g} simply reflect the fact that Δ_T^A dominates over Δ^E for A_{2u} and A_{1g} and that Δ^E is large and positive for B_{1g}.

E. B_{1g} and the Pressure-Induced Phase Transition

The relatively large decrease in $\omega(B_{1g})$ with pressure has important implications relative to the known occurrence of pressure-induced phase transitions in rutile as well as in other crystals having the rutile structure. Evidence for such transitions in rutile has come from shock-wave stress vs volume measurements[32] as well as from quasihydrostatic x-ray diffraction[33] and Raman-scattering[28] measurements. The shock results indicated a transition with a large volume change commencing slightly below 200 kbar, whereas the Raman work showed a transition at pressures above ~26 kbar. It is not known if the high-pressure phases are identical. The crystal structure of the high-pressure phase(s) and other properties of the transition(s) are not sufficiently known at present to allow anything but speculative comments about the lattice dynamical nature of the transition(s).

Nicol and Fong[28] suggested that the transition they observed above 26 kbar may be to the orthorhombic ($D_{2h}^{14} - Pbcn$) structure. Recently, Nagel and O'Keeffe[34] argued against this assignment and suggested instead that it may be an ortho-

rhombic ($D_{2h}^{12}-Pnnm$) $CaCl_2$ structure, and furthermore that this phase is made stable in the experiments by the presence of nonhydrostatic stresses. A transition to the $CaCl_2$ structure is attractive from the standpoint of the observed softening of B_{1g} with pressure. An examination of the rutile and $CaCl_2$ structures[34] suggests that the pattern of ionic displacements associated with B_{1g} (see Fig. 1) can lead to a transition to the $CaCl_2$ structure as $\omega(B_{1g})\to 0$. There is no requirement, however, that the soft-mode frequency precisely vanish for a transition to take place if the transition is of first order.[35] Theoretical considerations[30] show that only for a second-order transition does the frequency of the pertinent mode vanish at the transition, and furthermore, for such a transition only one normal mode can be involved. For a first-order transition, on the other hand, generally more than one mode may be involved and none of their frequencies vanish at the transition. In rutile our hydrostatic pressure data show that the decrease of $\omega(B_{1g})$, although relatively large, is only $0.24\%\,\mathrm{kbar}^{-1}$. Nicol and Fong obtained a decrease of $\sim 0.21\%\,\mathrm{kbar}^{-1}$, so that any nonhydrostatic effects in their experiments do not appear to significantly affect this shift. The experimental results show that a rather high pressure is needed for $\omega(B_{1g})\to 0$. Nonetheless, the observed pressure-induced transition may indeed by to the $CaCl_2$ structure and driven by the softening of B_{1g}. If so, the transition is of first order. It appears spread over a range of pressure in the Nicol and Fong experiment possibly due to the presence of pressure gradients and a slow rate of transformation.

Reference to Fig. 1 shows that the ionic displacements associated with B_{1g} consist of a rotation of the oxygen ions about an axis (c axis) through the Ti ions. The mode softens with both increasing pressure and decreasing temperature, though only slightly in the latter case. It is of interest to note that rotations of octahedral groups in the perovskites are known to play important roles in the temperature-induced phase transitions that are observed in these crystals.[36] For example, the 105 °K transition in $SrTiO_3$ is caused by the softening of the Γ_{25} phonon mode at the [111] zone boundary, and similarly the 184 and 88 °K transitions in $KMnF_3$ result from the softening of Γ_{25} and the [110] zone boundary phonon M_3, respectively.[37] Both Γ_{25} and M_3 involve rotations of the octahedral groups about an axis through the central ion. Such rotations are also believed to play a role in the transition in the antiferroelectric perovskites,[38,39] such as $PbZrO_3$, although in these cases the transitions are more complicated than that in $SrTiO_3$. It is noteworthy that the pertinent modes in these crystals soften with pressure as evidenced by an increase in the transition temperature T_t. For example, for $PbZrO_3$, $T_t = 507$ °K and $dT_t/dP = 4.5\,^{\circ}\mathrm{K\,kbar}^{-1}$.[39] Writing

$$\omega^2 \sim (T - T_t) \tag{17}$$

yields

$$\frac{\partial \ln\omega}{\partial P} = -\frac{1}{2}\left(\frac{\partial \ln T_t}{\partial P}\right) = -0.44\%/\mathrm{kbar}\ , \tag{18}$$

a value quite comparable to the present -0.24% kbar^{-1} for $\omega(B_{1g})$ of rutile, especially when account is made of the fact that $PbZrO_3$ is over twice as compressible as rutile.

F. Effective Ionic Charge e^*

On the basis of the results and data given in this paper it is possible to calculate the effective ionic charge e^* in rutile. For ionic crystals, e^* is generally calculated from the Szigeti equation,[40] which for a triatomic crystal with two identical ions, such as TiO_2, takes the form

$$\epsilon - \epsilon_\infty = \frac{4\pi(Ze^*)^2}{v\omega_{\mathrm{TO}}^2}\left(\frac{1}{m_1}+\frac{1}{2m_2}\right)\left(\frac{\epsilon_\infty+2}{3}\right)^2 \equiv \eta\ , \tag{19a}$$

where the right-hand side is denoted by η. Here $\epsilon-\epsilon_\infty$ is the lattice contribution to the static dielectric constant, v is the volume per molecule, ω_{TO} is the ir resonance frequency in rad/sec ($\equiv$ the soft-mode frequency ω_f in rutile for measurements along the c axis), Z is the valence ($=4$ for rutile), m_1 and m_2 are the masses of the Ti and O ions, respectively. Equation (19a) is derived in the harmonic approximation. For rutile, as seen earlier, the anharmonic contributions to the ϵ are large for $T \gg 0$ (see Fig. 4). In the high-temperature limit, these anharmonic contributions (denoted by G) can be accounted for by rewriting Eq. (19a) in the form[40]

$$\epsilon - \epsilon_\infty = \eta + G\ . \tag{19b}$$

The contribution G is given by

$$G = T\left(\frac{\partial(\epsilon-\epsilon_\infty)}{\partial T}\right)_V \approx T\left(\frac{\partial\epsilon}{\partial T}\right)_V \tag{20}$$

and can be evaluated directly from the data in Table II. All of the quantities in Eqs. (19) are thus known or can be evaluated from experimental data except e^* which can then be readily calculated.

At 4 °K the only anharmonicities contributing to the measured values of ϵ_c and ω_f of rutile are those associated with zero-point motion, and, as seen earlier, they are quite small. Thus, to a good approximation, the measured values of ϵ_c and ω_f can be taken to represent the strictly harmonic values, and Eq. (19a) can be used to calculate e^*. Using the 4 °K values, $\epsilon_c = 255$, $\epsilon_{\infty,c} = 7.2$,[41] $v = 31.05$ Å^3 ($\equiv \frac{1}{2}$ the unit cell volume), $\omega_f = 142$ cm^{-1}

$= 2.68 \times 10^{13}$ rad/sec, we obtain $e^*/e = 0.64$, where e is the electronic charge ($= 4.80 \times 10^{-10}$ esu).

At higher temperatures G becomes finite and e^* can be determined from Eq. (19b). Equation (20) for G is a high-temperature approximation and should be valid only for $T \geq \Theta_D$; however, since our earlier discussion suggested that rutile exhibits "high-temperature response" at $T \ll \Theta_D$, let us for the moment assume that Eq. (20) is valid at 296 °K, the highest T for which $\epsilon_c(T)$ data are available. On this basis the data in Table II yield $G = -66$. This represents the total anharmonic contribution to $\epsilon_c - \epsilon_{\infty,c}$ with the exception of the anharmonic effect associated with zero-point motion (assumed small) and the effect of thermal-expansion contained in η. The appropriate value of ω_f to use in the expression for η in Eq. (19b) is not the measured value at 296 °K ($= 172$ cm^{-1}) but the strictly harmonic value $\omega_{f,h}$ (neglecting zero-point motion effects) modified by the effect of thermal expansion. This is evaluated from the ω_f value at 4 °K ($= 142$ cm^{-1}) and the Δ^E data in Fig. 9 to yield 136 cm^{-1} for $\omega_{f,h}$ at 296 °K. Using these values of $\omega_{f,h}$ and G along with $\epsilon_c = 166.7$, $\epsilon_{\infty,c} = 7.2$, and $v = 31.20$ Å^3, Eq. (19b) yields $e^*/e = 0.58$. This is substantially smaller than the above value of 0.64 determined at 4 °K. However, in view of the assumptions invoked in determining G, some uncertainty exists as to whether the indicated T dependence of e^* is real.

A more accurate way of determining e^* at high temperature for soft-mode materials such as rutile is suggested by our earlier discussion. In Sec. IV B it was shown that, via the LST relation, $\epsilon_c = k'/\omega_f^2$, where k' is a constant independent of T. Thus, the anharmonic contributions to ϵ_c should be reflected faithfully in ω_f^2 and e^* can be accurately determined at any T from Eq. (19a) using the *measured values* of ϵ_c and ω_f at that T. At 296 °K the measured values are $\epsilon_c = 166.7$ and $\omega_f = 172$ cm^{-1}. Equation (19a) then yields $e^*/e = 0.62$. This is also lower than the 4 °K value, and we believe that the decrease in e^* with increasing T is real. A qualitative explanation follows.

In the ideal case of deformable ions which do not overlap, e^*/e is unity. In real crystals, however, the ions overlap, and the concept of an effective charge was introduced into the theory to account for the polarization effects associated with this overlap.[40,42] Deviations of e^*/e from unity arise from two effects: (i) short-range repulsive interactions between the electron clouds on adjacent ions which modify the electronic dipole moments and (ii) redistribution of charge and overlap when the ions move in the course of lattice vibrations. Both effects are apparently large in rutile leading to the relatively small value of e^*/e. This conclusion supports our earlier remarks concerning the possible explanation of the large value of A in Eq. (1) (see Sec. IV A 1). Increased anharmonic interactions with increasing temperature can be expected to result in additional distortion of the electron clouds and thus a decrease in e^* as indicated by the above calculations.

The present values of e^*/e can be compared with recent determinations by other authors. Traylor *et al.*,[5] by fitting their room-temperature neutron scattering data of the complete phonon dispersion curves to either a shell model or a rigid-ion model, obtained $e^*/e = 0.63$ and 0.55, respectively. Neither model provided a good over-all fit, but the shell model was better for some modes. Katiyar and Krishnan[43] fit $q \approx 0$ data for the optic modes to a rigid-ion model and found $e^*/e = 0.62$. We also note in passing that Szigeti's early calculations[40] using Eq. (19a) yielded $e^*/e = 0.65$. This result is fortuitous however, since it was obtained by using the then available, and inaccurate values of $\omega_f = 200$ cm^{-1}, $\epsilon_c = 173$, and $\epsilon_{\infty,c} = 8.42$. As shown above, the correct values of the parameters yield $e^*/e = 0.62$ at 296 °K.

The agreement in e^*/e reported by different authors is quite good with the exception of the 0.55 value from the fit to the dispersion curves assuming a rigid-ion model. Differences of the magnitude indicated are not surprising because both the rigid-ion and shell models are in reality rough approximations to a complicated lattice dynamical system. We also emphasize that our present values of e^*/e represent the so-called Szigeti effective charge—a "transverse" effective charge in that it relates to a transverse mode.

V. SUMMARY AND CONCLUSIONS

The main results and conclusions of this work can be summarized as follows.

(i) The static dielectric constants ϵ_a and ϵ_c of rutile are large and decrease with increasing temperature obeying a modified Curie–Weiss equation of the form first derived by Barrett. The parameters in this equation and their pressure dependence are evaluated and discussed. The temperature-independent parameter A is found to be large, and this is attributed to large electronic polarizabilities and to contributions to the ionic polarizability from nonpolar optic vibrations.

(ii) Comparison of the dielectric results with recent neutron scattering data shows that the large increase in ϵ_c on cooling is almost completely due to a decrease in the frequency of the soft optic (ferroelectric) mode A_{2u}. The pressure dependence of $\omega(A_{2u})$ is deduced and the Grüneisen parameter γ of this mode calculated. It is found that $\gamma(A_{2u})$ is large and increases strongly with decreasing temperature—unique properties of the FE mode.

(iii) The pressure and temperature dependences of the frequencies of the Raman-active modes B_{1g}, E_g, and A_{1g} were measured. In addition to A_{2u}, the modes B_{1g} and A_{1g} are anomalous in that their ω's increase with increasing T, though the changes are very small. Mode B_{1g} is especially anomalous in that, unlike all of the other modes, $\omega(B_{1g})$ *decreases* with pressure resulting in a relatively large and negative $\gamma(B_{1g}) = -5.0$. The possible connection between this result and the pressure-induced phase transition in rutile is discussed.

(iv) The pressure and temperature dependences of the dielectric constants and frequencies are combined to evaluate the pure-volume and pure-temperature contribution to each quantity. The latter contribution arises from cubic and quartic anharmonicities. It dominates the anharmonic self-energy shift of the soft A_{2u} mode and accounts for 20% of the mode energy at 300 °K. The two contributions are nearly equal in magnitude but opposite in sign for modes B_{1g} and A_{1g}, thus explaining the very weak isobaric T dependence of ω for these modes.

(v) The Szigeti effective ionic charge ratio for rutile is determined and found to be $e^*/e = 0.64$ at 4 °K and 0.62 at 296 °K. These results are discussed briefly.

ACKNOWLEDGMENTS

The authors deeply acknowledge the expert technical assistance of B. E. Hammons and M. J. Fitch in performing most of the measurements and wish to thank Dr. F. A. Mauer of the National Bureau of Standards for kindly providing the thermal-expansion data and Dr. J. G. Traylor for providing his neutron-determined $\omega(T)$ data for the soft A_{2u} mode. We are also grateful to Dr. N. S. Gillis for helpful discussions.

---

*Work supported by the U. S. Atomic Energy Commission.

[1]R. A. Parker, Phys. Rev. 124, 1719 (1961), and references therein.

[2]A. S. Barker, Jr. and M. Tinkham, J. Chem. Phys. 38, 2257 (1963); W. G. Spitzer, R. C. Miller, D. A. Kleinman, and L. E. Howarth, Phys. Rev. 126, 1710 (1962).

[3]S. P. S. Porto, P. A. Fleury, and T. C. Damen, Phys. Rev. 154, 522 (1967).

[4]M. H. Manghnani, J. Geophys. Res. 74, 4317 (1969); J. Reintjes and M. B. Schulz, J. Appl. Phys. 39, 5254 (1968).

[5]J. G. Traylor, H. G. Smith, R. M. Nicklow, and M. K. Wilkinson, Phys. Rev. B 3, 3457 (1971).

[6]B. Dayal, Proc. Indian Acad. Sci. 32A, 304 (1950); P. S. Narayanan, *ibid.* 37A, 411 (1953).

[7]A. VonHippel, J. Kalnajs and W. B. Westphal, J. Phys. Chem. Solids 23, 779 (1962). See also H. B. Lal and K. G. Srivastava, Can. J. Phys. 47, 3 (1969); O. W. Johnson *et al.*, J. Appl. Phys. 43, 807 (1972).

[8]B. E. Hammons, Rev. Sci. Instr. 42, 1889 (1971).

[9]J. S. Dugdale, Nuovo Cimento Suppl. 9, 27 (1958).

[10]J. E. Schirber, in *Physics of Solids at High Pressures*, edited by C. T. Tomizuka and R. M. Emrick (Academic, New York, 1965), p. 46.

[11]O. Brafman, S. S. Mitra, R. K. Crawford, W. B. Daniels, C. Postmus, and J. R. Ferraro, Solid State Commun. 7, 449 (1969).

[12]R. K. Kirby, J. Res. Natl. Bur. Std. 71A, 363 (1967).

[13]See, e.g., B. Morosin and G. A. Samara, Ferroelectrics 3, 49 (1971).

[14]J. H. Barrett, Phys. Rev. 86, 118 (1952).

[15]W. R. Abel, Phys. Rev. B 4, 2696 (1971).

[16]S. C. Abrahams and J. L. Bernstein, J. Chem. Phys. 55, 3206 (1971). See also T. W. Wyckoff, *Crystal Structures* (Wiley, New York, 1963), Vol. 1, p. 250.

[17]G. A. Samara, Ferroelectrics 2, 277 (1971).

[18]N. S. Gillis, Solid State Commun. 10, 887 (1972). A more detailed description of the model is given in Phys. Rev. B 4, 3971 (1971).

[19]The separation of the temperature dependence of the ϵ_i's of rutile into a pure volume and a pure temperature contribution, i.e., writing $\epsilon_i = \epsilon_i(V, T)$, involves an important assumption, but one that can be reasonably well justified in this case. Rutile is tetragonal, and therefore anisotropic, so that the ϵ_i's are functions of the axial ratio c/a in addition to being functions of volume. Uniaxial strain measurements are additionally needed to assess the effects of variations in c/a and these are difficult and not available. Our assumption is that the effects associated with the change in c/a with temperature are much smaller than those associated with the corresponding change in volume and are therefore negligible. Several factors suggest that this assumption should be quite good for rutile: (i) The fractional decrease in volume between 298 and 4 °K (= 0.44%) is 12.9 times larger than the corresponding decrease in c/a (= 0.034%). (ii) The fractional change in volume with pressure at constant T is five times larger than that in c/a. In view of these remarks we expect this assumption to be quite good for treating the temperature dependences of ϵ_a and ϵ_c as well as that of the frequency of the soft phonon mode A_{2u}. This conclusion is further supported, as will be shown later, by the fact that the isobaric temperature dependences of these quantities are strongly dominated by the pure temperature (i.e., volume-independent) effect, so that the pure volume effect is small. Since we expect the effect associated with the change in c/a to be even smaller than the volume effect, its neglect should not affect the conclusions significantly. In view of (i) and (ii) above we also expect the assumption to be quite satisfactory for analyzing the isobaric temperature dependences of the frequencies of the Raman active modes (see Sec. IV C).

[20]W. Cochran, Phys. Rev. Letters 3, 412 (1959); Advan. Phys. 9, 387 (1960).

[21]G. A. Samara, in *Advances in High Pressure Research*, edited by R. S. Bradley (Academic, New York, 1969), Vol. 3, Chap. 3; Phys. Rev. 151, 378 (1966). See also, W. N. Lawless and H. Gränicher, *ibid.* 157, 440, (1967).

[22]T. A. Davis and K. Vedam, J. Opt. Soc. Am. 58, 1446 (1968); S. Ramaseshan, K. Vedam, and R. S.

Krishman, in *Progress in Crystal Physics*, edited by R. S. Krishman (S. Viswanathan, Madras, 1958), Chap. V.

[23]A. S. Barker, Jr., Phys. Rev. 136, A1290 (1964).

[24]P. A. Fleury and J. M. Worlock, Phys. Rev. 174, 613 (1968).

[25]G. Shirane, R. Nathans, and V. J. Minkiewicz, Phys. Rev. 157, 396 (1967).

[26]G. A. Samara, Ferroelectrics 2, 177 (1971).

[27]J. M. Worlock, in *Structural Phase Transitions and Soft Modes*, edited by E. J. Samuelsen, E. Andersen, and J. Feder (Universitetsforlaget, Geilo, Norway, 1971), p. 329.

[28]M. Nicol and M. Y. Fong, J. Chem. Phys. 54, 3167 (1971).

[29]A. A. Maradudin and A. E. Fein, Phys. Rev. 128, 2589 (1962).

[30]R. A. Cowley, Phil. Mag. 11, 673 (1965); Advan. Phys. 12, 421 (1963).

[31]R. P. Lowndes, Phys. Rev. Letters 27, 1134 (1971); J. Phys. C 4, 3083 (1971).

[32]R. K. Linde and P. S. DeCarli, J. Chem. Phys. 50, 319 (1969).

[33]J. C. Jamieson and B. Olinger, Science 161, 893 (1968).

[34]L. Nagel and M. O'Keeffe, Mater. Res. Bull. 6, 1317 (1971).

[35]G. A. Samara, Phys. Rev. B 2, 4194 (1970).

[36]P. A. Fleury, J. F. Scott, and J. M. Worlock, Phys. Rev. Letters 21, 16 (1968).

[37]V. J. Minkiewicz and G. Shirane, J. Phys. Soc. Japan 26, 674 (1969).

[38]W. Cochran and A. Zia, Phys. Status Solidi 25, 273 (1968).

[39]G. A. Samara, Phys. Rev. B 1, 3777 (1970).

[40]B. Szigeti, Discussions Trans. Faraday Soc. 45, 155 (1949); Proc. Roy. Soc. (London) A252, 217 (1959); A261, 274 (1961).

[41]J. R. DeVore, J. Opt. Soc. Am. 41, 418 (1951). The appropriate value of $\epsilon_{\infty,c}$ to use in Eqs. (19) is the long-wavelength limiting value of 7.2 and not the generally quoted value of 8.4.

[42]B. G. Dick and A. W. Overhauser, Phys. Rev. 112, 90 (1958).

[43]R. S. Katiyar and R. S. Krishnan, Phys. Letters 25A, 525 (1967).